

Evolution of Compact Groups of Galaxies I. Merging rates

E. Athanassoula,¹ J. Makino,² and A. Bosma¹

¹*Observatoire de Marseille, 2 Place Le Verrier, F-13248 Marseille Cedex 4, France*

²*Department of Information Science and Graphics, College of Arts and Sciences, The University of Tokyo, Tokyo 153, Japan*

Accepted . Received ; in original form 1996 June

ABSTRACT

We discuss the merging rates in compact groups of 5 identical elliptical galaxies. All groups have the same mass and binding energy. We consider both cases with individual halos and cases where the halo is common to all galaxies and enveloping the whole group. In the latter situation the merging rate is slower if the halo is more massive. The mass of individual halos has little influence on the merging rates, due to the fact that all galaxies in our simulations have the same mass, and so the more extended ones have a smaller velocity dispersion. Groups with individual halos merge faster than groups with common halos if the configuration is centrally concentrated, like a King distribution of index $\Psi = 10$. On the other hand for less concentrated configurations the merging is initially faster for individual halo cases, and slower after part of the group has merged. In cases with common halo, centrally concentrated configurations merge faster for high halo-to-total mass ratios and slower for low halo-to-total mass ratios. Groups whose virial ratio is initially less than one merge faster, while groups that have initially cylindrical rotation merge slower than groups starting in virial equilibrium.

In order to test how long a virialised group can survive before merging we followed the evolution of a group with a high halo-to-total mass ratio and a density distribution with very little central concentration. We find that the first merging occurred only after a large number of crossing times. A reasonable calibration of our computer units shows that this time should be larger than a Hubble time. Therefore, our simulations suggest that, at least for appropriate initial conditions, the longevity of compact groups is not necessarily a problem, thus presenting an alternative explanation to why we observe so many compact groups despite the fact that their lifetimes seem short.

Key words: galaxies: interactions – galaxies: structure – galaxies: kinematics and dynamics.

1 INTRODUCTION

Hickson compact groups (hereafter HCGs) are tight associations of at least four galaxies fulfilling specific criteria concerning their compactness and isolation. Hickson (1982), using the Palomar sky survey prints, catalogued 100 such systems of which 92 were subsequently found to contain at least three members with accordant redshifts (Hickson *et al.* 1992). The observed projected separations imply very high space densities, equal to or greater than those found in the cores of clusters of galaxies, while their velocity dispersions are moderate (Hickson *et al.* 1992), of the same order as velocity dispersions in bright galaxies. This makes them ideal sites for interactions and mergings. Thus the question of why such groups are still observed and have not merged already arises naturally. Either for some reason the relevant time-

scales for their merging are longer than expected, or compact groups are a relatively short lived evolutionary phase in a frequently occurring scenario, or they are not real configurations but chance projections.

Barnes (1985) considers the possibility that a common dark halo might envelop a compact group and shows with the help of N body simulations that this slows down the merging process. His groups are constituted of 5 to 10 elliptical galaxies and each galaxy is represented by 75 or 100 mass points. His conclusion has been corroborated by the work of Navarro, Mosconi & Garcia Lambas (1987) and Cavaliere *et al.* (1982), although those simulations do not strictly pertain to compact groups and are made with much fewer particles. More recently Bode, Cohn & Lugger (1992), using a total of 5000 particles and King laws for all mass distributions (mass within a given galaxy, distribution of galaxies in the

group and distribution of mass within the common halo), come to the same conclusion as Barnes. On the other hand Athanassoula and Makino (1995), using Plummer laws for all the mass distributions, found that the complete merging of the group into one object happens earlier in cases with common halos than in cases of individual halos with the same distribution as the light component.

Thus, although the amount and distribution of dark will influence the merging times, it is not clear exactly how. Other factors such as the distribution of the galaxies in the group, or their kinematics, have not yet been fully investigated. In this paper we return to the problem, using a larger number of particles and, in particular, trying more simulations with different distributions, in order to understand if and how these distributions influence the merging rates. Our simulations are presented in section 2 and the criterion for merging in section 3. Some general information on the evolution of the runs is given in section 4. Merging rates are compared in section 5. Section 6 discusses pairs and triplets. A general discussion is given in section 7, where we also present one simulation which takes a long time before merging.

2 SIMULATIONS

2.1 Galaxy models

To simplify the problem, we have modelled all galaxies constituting a group as ellipticals. This results in savings on both the number of particles and the amount of simulations to be performed, since more particles are necessary to model disc galaxies, and the relative orientation of these discs can influence the merging rates (White 1979, Barnes 1992). Furthermore all galaxies constituting the group are taken to be identical (simulations of groups with unequal mass galaxies have been reported by Governato, Bhatia & Chincarini (1991), by Weil & Hernquist 1994 and 1996, and by Athanassoula & Makino (1995)). Thus our individual galaxy models will represent ellipticals with or without individual halos, and different masses and sizes will be considered for the halo component. To enable meaningful comparisons, we have ensured that the radial dependences of the density of the luminous material of all the galaxy models are as similar as possible. This is of course only approximate, since a figure in equilibrium in a halo is not the same as a figure in equilibrium in its own gravitational potential. Our setup procedure, however, ensures considerable similarity.

The galaxies are modelled as Plummer spheres or, in the case of galaxies with halos, as composite models represented by two superposed Plummer spheres which are evolved together to equilibrium*. More specifically, we have used five galaxy models, denoted in Tables 1, 2 and 3 by g0, g1, g2, g3 and g4. Model g0 represents a halo-less elliptical and is modelled by a simple Plummer sphere. Model g1 represents an

* An alternative, and certainly more elegant, way of constructing composite models is to calculate, if possible, analytical distribution functions of such systems, as done recently by Ciotti (1996) for a Hernquist model in a Hernquist halo

Table 1. Global parameters for individual galaxies

galaxy	M_{ch}/M_t	M_{ih}/M_t	E	$\sqrt{2 E /M}$
g0	0.5	0.	-0.98	0.99
g0	0.75	0.	-0.24	0.69
g0	0.875	0.	-0.06	0.50
g1	0.	0.5	-2.71	1.16
g2	0.	0.5	-2.20	1.05
g3	0.	0.75	-1.49	0.86
g4	0.	0.875	-0.82	0.64

Table 2. Radii for individual galaxies

galaxy	$r(.3)$	$r(.8)$	$r_l(.3)$	$r_l(.8)$	$r_h(.3)$	$r_h(.8)$
g0	0.5	1.5	0.5	1.5	—	—
g1	0.7	2.7	0.5	1.7	1.0	3.6
g2	0.8	3.9	0.5	1.6	1.6	6.1
g3	1.2	5.5	0.5	1.5	1.9	6.5
g4	2.4	9.4	0.5	1.6	3.1	10.

elliptical with a halo of relatively short extent and has been constructed in the following way: We create two Plummer spheres of equal mass, each with 2048 particles. We rescale one in radius by a factor of 0.5 and call, for simplicity, the extended component the halo and the less extended one the luminous part. Then we evolve the composite configuration for a time interval sufficient to reach equilibrium. Keeping its energy constant, we now rescale this model so that the half-mass radius of the luminous part is equal to that of the simple Plummer model and its mass equal to that of the simple Plummer model g0 used in simulations with common halos and the same halo-to-total mass ratio.

Model g2 was built in exactly the same way as g1 except that the ratio of the extents of the two components is taken to be 0.25, instead of 0.5, thus aiming for a halo of larger extent compared to the optical part. Model g3 has a halo which is three times more massive than the luminous part and is initially four times as extended. Finally the halo of model g4 is seven times more massive than the optical part and is initially eight times more extended. Before being used in the group simulations, all composite models were evolved for 30 time units, an ample time for equilibrium between the two components to be reached.

Table 1 gives some properties of the galaxies we have used. Column 1 gives the name of the galaxy, in the notation introduced above, columns 2 and 3 its halo-to-total mass ratio (for the common and individual halos respectively), column 4 its binding energy and column 5 a measure of its velocity dispersion. The density profiles of the evolved galaxies are compared in Table 2. Columns 1 and 2 give the radii containing 30% and 80% of the total galaxy mass, columns 3 and 4 the same radii for the luminous mass, and columns 5 and 6 for the halo. We note that the luminous parts of the three configurations are quite similar, as desired. The total density distribution of the models with halos is considerably more extended than that of model g0, while models g1 and g2 differ mainly in their outer parts. We note that

the characteristic radii of composite models are somewhat smaller than those of their unevolved halos, as a result of the additional pull inwards from the luminous part.

2.2 Models for the distribution of galaxies in the group and for the common halo

Each group is initially constituted of 5 identical galaxies whose initial positions and velocities are drawn randomly from a distribution which is either a Plummer model or a King model of a given index. Only King models with indexes $\Psi = 1, 5$ or 10 have been used. The concentration of the King models increases with their index Ψ . Thus the $\Psi = 10$ distribution is the most centrally concentrated one, while having an extended outer part. The intermediate case $\Psi = 5$ is rather similar to the Plummer distribution. Five realisations of each of these four distributions have been made and used identically both for the simulations with common halos and for the ones without.

The models for the common halo distribution have also been chosen to be either Plummer models or King models with indexes $1, 5$ or 10 . For simplicity, and to keep the number of simulations limited, in all our models the halo mass is either in individual galactic halos or in common halos. No cases with part of the mass in one type of halo and part of the mass in the other have been considered. Three different fractions of halo mass have been considered, corresponding to $M_{lum}/M_{tot} = 0.5, 0.25$ or 0.125 , where M_{lum} is the mass in the luminous parts of the galaxies and M_{tot} is the total mass in the simulation.

Most of our simulations start off with a virial ratio $2T/|W|$ equal to 1 and random orientations of the velocity vectors. Nevertheless the models where the distribution for the group and the halo are not of the same type will start off equilibrium. We have also run 70 simulations of Plummer groups in (whenever relevant) Plummer halos with different initial kinematics. For reasons that will be discussed in the following sections, all but five had a $M_{lum}/M_{tot} = 0.125$, the remaining five having a $M_{lum}/M_{tot} = 0.5$. We experimented with cylindrically rotating, cold and expanding groups. For the rotating ones we proceed as follows. We first create the group in virial equilibrium and then add rotation in the (x, y) plane by setting the velocity in that plane to be perpendicular to the position vector in that plane. This means that we give these models the maximum possible velocity around the z axis without any change in their z -component of velocity and their kinetic energy. Cold groups have a virial ratio $2T/|W| = 0.25$ or 0.5 , while having the same total energy and mass as the ones in virial equilibrium. Finally for the expanding groups the galaxy bulk-velocity vectors are oriented such that there is only expansion, their amplitude is taken to be proportional to the distance of the galaxy from the center of the group, while the total mass and energy are kept constant. The same procedure is also followed, whenever relevant, for the common halo, except that now we eliminate the halo particles that are unbound.

The principal characteristics of the simulations discussed in this paper are listed in Table 3. Many more simulations were run than those listed. Since, however, they did not add new substantial information, or only corroborated results already obtained with other simulations, they will not be listed or discussed here. The first column gives the names

of the runs, the second the model used for the galaxy and the third the model used for the group. The fourth gives the model for the common halo, a dash indicating that there was no common halo, and the fifth column gives the ratio of halo-to-total mass. The sixth one gives information on the kinematics of the initial configuration. *Virial* denotes groups for which $2T/|W| = 1$ and *cold* groups with $2T/|W| = 0.25$ or 0.5 , in both cases the direction of the velocity vector being chosen at random. *Rotating* groups also have $2T/|W| = 1$, but now the component of the velocity perpendicular to the z axis has been put in a direction perpendicular to the distance of the galaxy from the z axis. Finally *exp* denotes groups expanding with a uniform Hubble flow. The seventh column gives the number of particles in each galaxy and the eighth one the total number of particles in the simulation. The number of particles in each component has been chosen such that the mass of the particles constituting the luminous part is equal to that of the particles constituting the halo. Missing identification numbers refer to runs which are not essential for the discussions in this paper.

2.3 Numerical miscellanea

In our units $G = 1$ and the total mass of the group is equal to 20 for all models. In the case of groups with no common halo the binding energy of the group, excluding the internal binding energy of the galaxies, is -5 . This is also approximately true for the cases with common halo. Therefore, the velocity dispersion within a group is $\sqrt{2|E|/M} = 1/\sqrt{2}$, where E and M are the binding energy and the total mass of the group.

Most of the numerical simulations have been carried out using direct summation on the GRAPE-3A and GRAPE-3AF boards in Marseille Observatory and a few on similar boards in Tokyo University (for description of GRAPE 3 boards see e.g. Okumura *et al.* 1992, Ebisuzaki *et al.* 1993 and Okumura *et al.* 1993). In the Marseille 3AF configuration one time-step takes 6.3 secs for simulations with 65400 particles. The time-step chosen is equal to 0.015625 , and the softening in most cases equal to 0.03125 . A few cases (namely runs King7 to King11 and King27 to King29) have been evolved with a softening of 0.025 , but that makes no difference to the evolution. These parameters ensure an adequate energy conservation. Thus on average the energy was conserved better than 0.1% up to $t = 100.$, better than 0.15% up to $t = 500.$ and better than 0.35% up to $t = 1000.$ (i.e. $64\ 000$ time-steps).

A number of the simulated groups took a long time before merging, and a few did not merge at all. It is thus of interest to ask whether the number of particles we use is sufficient to prevent our results from being severely influenced by two-body relaxation effects. The run which is most liable to be problematic is ki33 since it is modelled with 16350 particles, the lowest we have used in our simulations, and furthermore has not merged by $t = 1000.$ We thus reran this simulation with double the number of points (ki57) and compared the positions of galaxies as a function of time. Despite the length of the runs the positions of the galaxies in the two simulations agree on average better than 5% .

Table 3. List of runs

Run	Galaxies	Group	CH	M_{halo}/M_{tot}		N_g	N_s
pl54, pl47, pl48, pl49, pl50	g1	p	-	0.5	<i>virial</i>	4096	20480
pl55, pl17, pl51, pl52, pl53	g2	p	-	0.5	<i>virial</i>	4096	20480
pl56, pl22, pl23, pl24, pl25	g0	p	p	0.75	<i>virial</i>	1635	32700
pl27, pl28, pl29, pl30, pl31	g3	p	-	0.75	<i>virial</i>	4096	20480
pl37, pl38, pl39, pl40, pl41	g0	p	p	0.5	<i>virial</i>	1635	16350
pl42, pl43, pl44, pl45, pl46	g0	p	p	0.875	<i>virial</i>	1635	65400
pl57, pl58, pl59, pl60, pl61	g4	p	-	0.875	<i>virial</i>	4096	20480
ki2, ki3, ki4, ki5, ki6	g2	k5	-	0.5	<i>virial</i>	4096	20480
ki7, ki8, ki9, ki10, ki11	g1	k5	-	0.5	<i>virial</i>	4096	20480
ki12, ki13, ki14, ki15, ki16	g0	k5	k5	0.75	<i>virial</i>	1635	32700
ki17, ki18, ki19, ki20, ki21	g0	k10	k10	0.75	<i>virial</i>	1635	32700
ki22, ki23, ki24, ki25, ki26	g2	k10	-	0.5	<i>virial</i>	4096	20480
ki27, ki28, ki29, ki30, ki31	g1	k10	-	0.5	<i>virial</i>	4096	20480
ki32, ki33, ki34, ki35, ki36	g0	k10	k10	0.5	<i>virial</i>	1635	16350
ki37, ki38, ki39, ki40, ki41	g3	k10	-	0.75	<i>virial</i>	4096	20480
ki47, ki48, ki49, ki50, ki51	g0	k10	k10	0.875	<i>virial</i>	1635	65400
ki52, ki53, ki54, ki55, ki56	g4	k10	-	0.875	<i>virial</i>	4096	20480
ki59, ki60, ki61, ki62, ki63	g4	k1	-	0.875	<i>virial</i>	4096	20480
ki64, ki65, ki66, ki67, ki68	g0	k1	k1	0.875	<i>virial</i>	1635	65400
ki69, ki70, ki71, ki72, ki73	g0	k1	k1	0.5	<i>virial</i>	1635	16350
ki74, ki75, ki76, ki77, ki78	g3	k1	-	0.75	<i>virial</i>	4096	20480
ki79, ki80, ki81, ki82, ki83	g0	k1	k1	0.75	<i>virial</i>	1635	32700
ki84, ki85, ki86, ki87, ki88	g1	k1	-	0.5	<i>virial</i>	4096	20480
kp2, kp3, kp4, kp5, kp6	g0	k10	p	0.75	<i>virial</i>	1635	32700
kp7, kp8, kp9, kp10, kp11	g0	k10	p	0.5	<i>virial</i>	1635	16350
pk5, pk6, pk12, pk13, pk14	g0	p	k10	0.75	<i>virial</i>	1635	32700
pk10, pk11, pk15, pk16, pk17	g0	p	k10	0.5	<i>virial</i>	1635	16350
pl62, pl63, pl64, pl65, pl66	g4	p	-	0.875	<i>rotating</i>	4096	20480
pl67, pl68, pl69, pl70, pl71	g0	p	p	0.875	<i>rotating</i>	1635	65400
pl77, pl78, pl79, pl80, pl81	g0	p	p	0.875	<i>cold</i>	1635	65400
pl82, pl83, pl84, pl85, pl86	g4	p	-	0.875	<i>exp 0.5</i>	4096	20480
pl87, pl88, pl89, pl90, pl91	g1	p	-	0.5	<i>rotating</i>	4096	20480
pl92, pl93, pl94, pl95, pl96	g4	p	-	0.875	<i>cold 0.25</i>	4096	20480
pl97, pl98, pl99, pl100, pl101	g0	p	p	0.875	<i>cold 0.25</i>	1635	65400
pl107, pl108, pl109, pl110, pl111	g4	p	-	0.875	<i>cold 0.5</i>	4096	20480
pl112, pl113, pl114, pl115, pl116	g0	p	p	0.875	<i>cold 0.5</i>	1635	65400
pl122, pl123, pl124, pl125, pl126	g0	p	p	0.875	<i>exp 1.</i>	1635	65400
pl127, pl128, pl129, pl130, pl131	g4	p	-	0.875	<i>exp 1.</i>	4096	20480

3 CALCULATION OF MERGING RATES

To calculate merging rates we must first adopt a criterion determining when two galaxies merge. Barnes (1985) and Bode, Cohn & Lugger (1992) use a friends-of-friends algorithm, but this decides that two galaxies have merged from the moment their halos or their luminous parts (depending on whether we apply it to the total or only to the luminous mass distribution) have started to interpenetrate. Since parts of galaxies may overlap without them having merged, we believe that this criterion is not stringent enough, and we chose to associate merging with loss of identity. Thus two galaxies are considered merged if the distance between their centers is smaller than a given fraction of some characteristic radius, and the difference between their bulk velocities smaller than a given fraction of some associated characteristic velocity.

We use as comparison radii and velocities the minimum of the radii and velocity dispersions of the two galaxies, so that the adopted criterion reads:

$$R_{ij} < 0.5 \min(r_{g,i}, r_{g,j}) \quad (1)$$

$$V_{ij} < 0.5 \min(\sigma_i, \sigma_j) \quad (2)$$

where R_{ij} and V_{ij} are the relative distance and velocity between galaxies i and j , and $r_{g,k}$ and σ_k are the radius and central velocity dispersion of galaxy k . The center of each galaxy is defined as the position of the highest density, i.e. the average position weighted by the local density, or

$$\mathbf{r}_c = \frac{\sum_{i=1}^N \rho_i \mathbf{r}_i}{\sum_{i=1}^N \rho_i} \quad (3)$$

where \mathbf{r}_i is the position of particle i , ρ_i is the local density around particle i calculated using the six nearest neighbours and the sums are over all particles that initially belong to the galaxy. Similarly the characteristic radius of a galaxy is defined by:

$$r_g = \sqrt{\frac{\sum_{i=1}^N \rho_i r_i^2}{\sum_{i=1}^N \rho_i}} \quad (4)$$

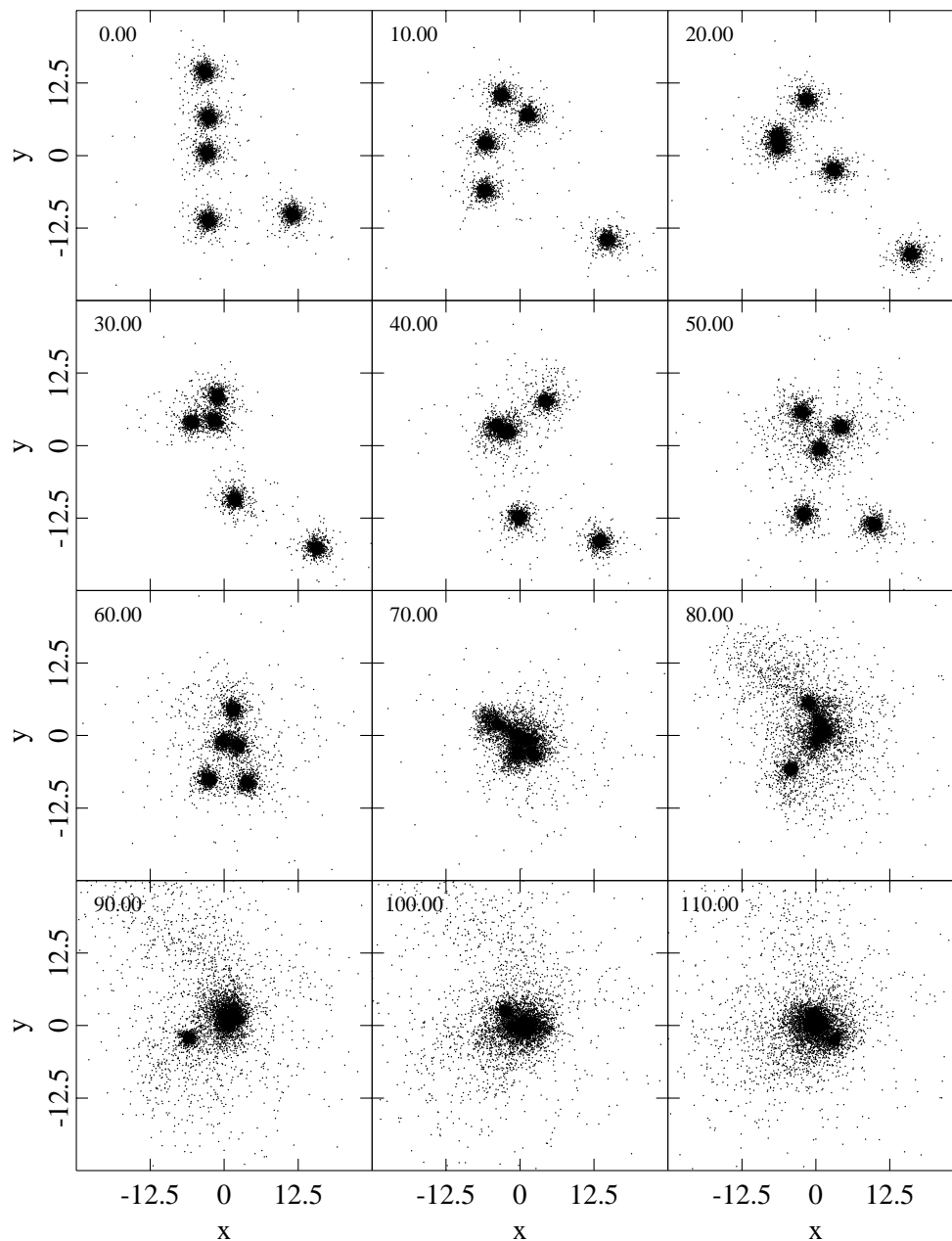


Figure 1. Evolution of model ki16. Time increases from left to right and from top to bottom and is given in the upper left corner of each frame. We plot the xy projection of all particles representing the luminous matter.

where ρ_i and the summation are defined as above, and r_i is the distance of particle i from the density center of each galaxy defined in eq. (3). Our definition is similar, but not identical, to that used by von Hoerner (1963) and Casertano and Hut (1985), since they use the average of the absolute distance weighted by the local density to calculate the radius, while we calculate the weighted root-mean-squared distance from the center. For the central velocity dispersion we take the root-mean-squared velocity of particles within a radius equal to twice r_g .

Roughly speaking, our procedure to find the size and the velocity dispersion of a galaxy is to look at the distribu-

tion of particles that are originally in that galaxy, mark the region with highest density and calculate the velocity dispersion within that region. To determine whether two galaxies have merged, we check if these high-density regions overlap sufficiently and if their relative velocity is small enough. Note that our procedure can be easily applied to galaxies which have already merged with other galaxies, since it does not use the binding energy. We were thus able to use this procedure to determine if all the five galaxies have formed one merger or not, just by looking at all the pairs.

This criterion performed very well in most cases. In only about 2% of the cases it came to unreasonable con-

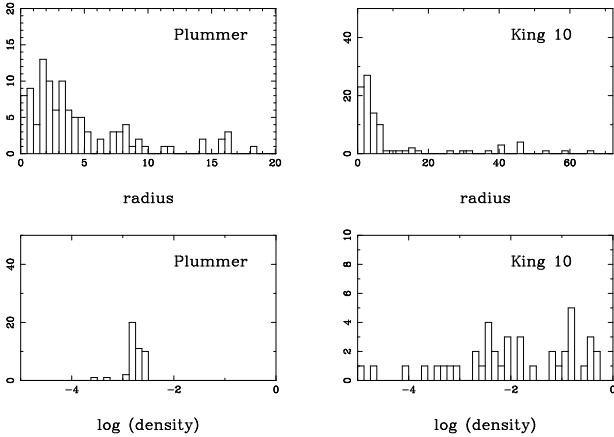


Figure 2. Information on where the first, second and third merging occurred. The upper panels give histograms of the distances of these locations from the center-of-mass of the group. The two lower ones give histograms of the density of the unperturbed common halo at the merging locations. The left panels correspond to Plummer groups and the right panels to King $\Psi = 10$ groups.

clusions, saying e.g. that galaxy 1 has merged with galaxy 2 and galaxy 3, but galaxies 1 and 3 had not merged between them. In yet fewer cases, less than 1%, the criterion declares two galaxies as having merged at a given time step, and not having merged in the next one. Such cases can be identified as temporary increases of the number of galaxies in Figures 3 to 9 and 11 to 12. This criterion was applied to every one of our runs and the results are compared in figures 3 to 9 and 11 to 12, which give the mean number of galaxies left in the group as a function of time. Since in all cases we average over 5 configurations, the number of galaxies is of course not be necessarily an integer. We repeated the exercise by applying the merging criterion to only the luminous part of the galaxies : our results for the merging rates stay the same independent of whether we consider the luminous part or the whole galaxy.

4 RESULTS

The evolution of a typical run is shown in Figure 1. The galaxies move within the group and interact. Part of the kinetic energy of their bulk motions is converted to internal motions and they suffer orbital decay. When they approach each other sufficiently close and with not too high relative velocity, they merge, until the group is reduced to only one object. The speed at which these mergings occur is to a large extent dependent on chance, via the randomly generated initial positions and velocities of the galaxies, but is also dependent on the global characteristics of the set-up, like the amount and distribution of dark matter, and in the following we will attempt to find out which factors determine this rate. In order to compensate to some extent for the element of chance every configuration was realised five times.

The positions where the mergings occur depend a lot on the initial configuration in the sense that they reflect the initial distribution of galaxies within the group, as is shown

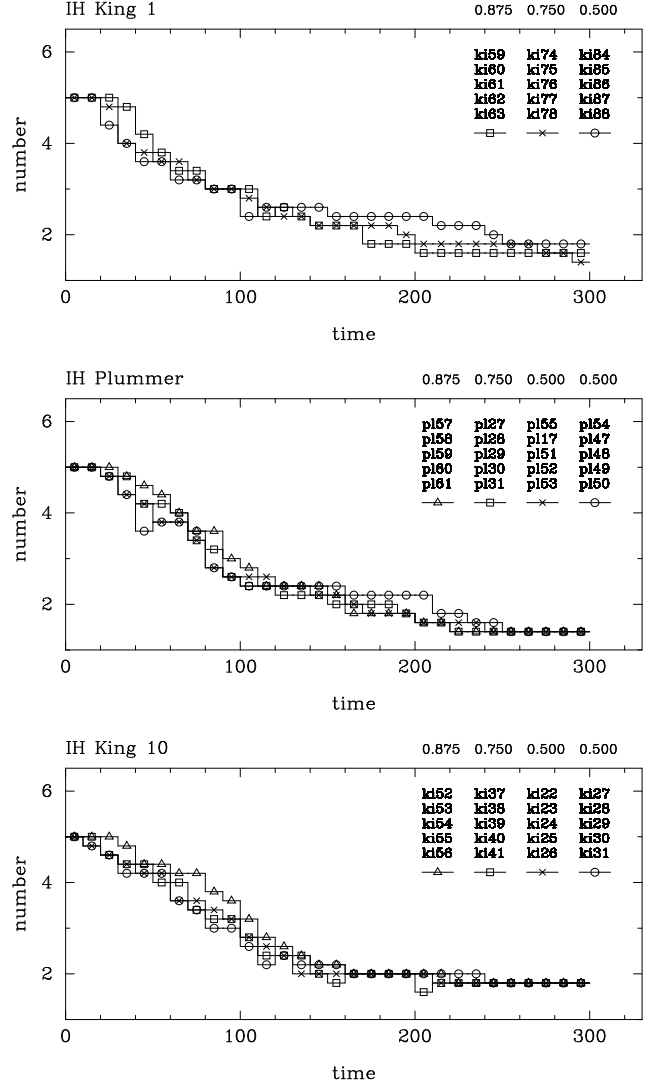


Figure 3. Number of galaxies as a function of time for groups with individual halos. The upper panel corresponds to King $\Psi = 1$ groups and shows the mean number of galaxies for groups with g1 galaxies (circles), groups with g3 galaxies (crosses) and groups with g4 galaxies (squares). The middle panel corresponds to Plummer groups and shows the mean number of galaxies for groups with g1 galaxies (circles), groups with g2 galaxies (crosses), groups with g3 galaxies (squares) and groups with g4 galaxies (triangles). The lower one corresponds to King $\Psi = 10$ groups and shows the mean number of galaxies for groups with g1 galaxies (circles), groups with g2 galaxies (crosses), groups with g3 galaxies (squares) and groups with g4 galaxies (triangles). The merging rates of the different groups can hardly be distinguished from each other, and this independent of the model of the group (King or Plummer).

in Figure 2. In order to obtain this figure we measured for each simulation the distance of the locations where the first, second and third mergings occurred from the center of mass of the group. The upper left panel of Figure 2 shows the number of mergings as a function of that distance for all simulations with a Plummer distribution starting off in virial equilibrium in (whenever relevant) a Plummer common halo.

The upper right panel has the same information, but now for King $\Psi = 10$ distributions starting off in virial equilibrium in (whenever relevant) King $\Psi = 10$ common halos. We note that in King $\Psi = 10$ distributions a lot of the mergings occur either very near the center or very far out, while in a Plummer distribution there are many more mergings at intermediate distances. This difference is also reflected in the lower panels of the same figure, where instead of the distance from the center of mass we have the density of the unperturbed common halo at the location of the merging. Thus these panels do not contain simulations with individual halos. In the Plummer case the densities are all concentrated in a narrow region of values, while in the King $\Psi = 10$ case both very high and very low densities are not uncommon. It seems that the distribution of galaxies in the group is the dominant factor in this case, and not the distribution of dark matter in the common halo, since mergings at very large distances from the group center of mass are also seen in the evolution of King $\Psi = 10$ groups in Plummer halos (kp series of runs), although our statistics are much poorer in this case.

Somewhat less than 90% of the mergings involve 2 galaxies, roughly 10% involve 3 galaxies and only about 1% involves 4 galaxies. In one case all 5 galaxies of the group merged in the same time-step. 90% of the pairs have a mass ratio 1:4 and 10% have a mass ratio 2:3. Roughly 75% of all triplets have a mass ratio 1:1:3, the remaining having a mass ratio 1:2:2.

5 COMPARING MERGING RATES

5.1 Individual halos

To compare merging rates for groups with individual halos of different masses and extents we plot in Figure 3 the number of galaxies left at any given time as a function of time. Surprisingly, the rates depend very little on the model galaxy used, even though the relative mass and the radial extent of the halos for galaxies g1, g2, g3 and g4 are quite different. This result holds for all types of groups tested, i.e. Plummer groups and King $\Psi = 1, 5$ or 10 groups. Table 1 shows that both the radii containing 30% and those containing 80% of the total galaxy mass are about a factor 3.5 larger for model g4 than for model g1. On the other hand, since the mass in each configuration, and therefore each galaxy, is the same, more extended configurations have a smaller absolute value of the binding energy and therefore a smaller value of $\sigma_{gal}/\sigma_{group}$ (cf columns 4 and 5 of Table 1). Therefore galaxy encounters happen at a smaller (relative to their internal dispersion) velocity in cases with less extended halos, and this will induce higher merging rates. Thus two counterproducing effects are at work : when galaxies become more extended their merging rates increase, but, since at the same time their internal velocity dispersion decreases, this decreases their merging rates as well. It is not possible to decouple the two effects, unless we consider a different number of galaxies at the start, or a different total mass, or galaxies that start out of equilibrium, all three alternatives being undesirable. For our simulations the two effects must be of about equal importance since the merging rates do not depend in a systematic way on the model

used. This can be seen in a more quantitative, albeit still very simple, way, as follows:

The probability that a given galaxy merges with another one in a unit time interval is expressed as

$$P = 4\pi \int_0^\infty f(v)n\sigma(v)v^3 dv, \quad (5)$$

where $f(v)$ is the distribution function of the relative velocity, n is the number density of galaxies and $\sigma(v)$ is the merging cross section for a given relative velocity. The cross section σ is actually also a function of the type of the galaxies. For simplicity, we here assume that galaxies are homologous, and therefore that the relation

$$r\sigma_{gal}^2 = \text{const.} \quad (6)$$

holds for different galaxies, where r is the characteristic radius of the galaxy (for example the virial radius) and σ_{gal} is its velocity dispersion. If we write the cross section explicitly as a function of v and r , we have, from dimensional analysis:

$$\sigma(v, r) = k^{-2}\sigma(vk^{-1/2}, kr). \quad (7)$$

Let us consider two groups consisting of galaxies of two different sizes, r_1 and $r_2 = kr_1$ respectively. We have

$$P_1 = 4\pi \int_0^\infty f(v)\sigma(v, r_1)v^3 dv,$$

$$P_2 = 4\pi \int_0^\infty f(v)\sigma(v, r_2)v^3 dv \\ = 4\pi k^2 \int_0^\infty f(v)\sigma(vk^{1/2}, r_1)v^3 dv \quad (8)$$

$$= 4\pi \int_0^\infty f(vk^{-1/2})\sigma(v, r_1)v^3 dv, \quad (9)$$

There are two limiting cases. In one case, the velocity dispersion within the cluster is much larger than the internal velocity dispersion of galaxies. Since the cross section becomes zero at $v \sim \sigma_{gal}$ (Makino and Hut 1996), we can, in this case, consider $f(v)$ to be independent of v , unless the velocity distribution function is singular at $v = 0$. We then have

$$P_2 \sim P_1. \quad (\sigma_{group} \gg \sigma_{gal}) \quad (10)$$

In other words, in the limit of $\sigma_{group} \gg \sigma_{gal}$, the merger rate, and therefore the lifetime of a group, does not depend on the size of the individual galaxies.

The other extreme is when the internal velocity dispersion of the galaxies is much larger than that of the cluster. In this case we need an asymptotic form of the cross section σ . Both numerical scattering experiments and approximate theory suggest that $\sigma \propto v^{-8/3}$ for small v (Makino & Hut, 1996). The gravitational focusing effect alone requires the power index to be larger than -2 (Makino & Hut 1996). Thus, we have

$$P_2 \sim k^{2/3}P_1 \quad (\sigma_{group} \ll \sigma_{gal}), \quad (11)$$

i.e. a weak dependence on k . Our simulations are of course intermediate between these two extreme cases. Furthermore

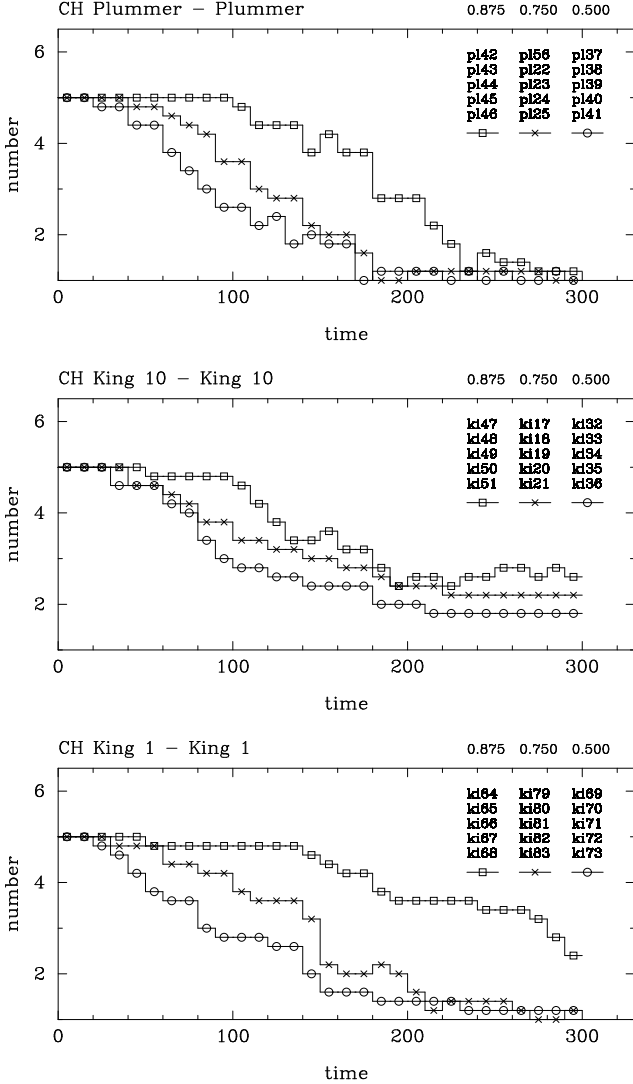


Figure 4. Number of galaxies as a function of time for groups with common halos. The upper panel corresponds to Plummer groups and common Plummer halos, and shows the mean number of galaxies for groups with 0.5 (circles), 0.75 (crosses) and 0.875 (squares) halo-to-total mass ratio. The middle panel corresponds to King $\Psi = 10$ groups in common King $\Psi = 10$ halos and the lower one to King $\Psi = 1$ groups in King $\Psi = 1$ common halos. The different symbols correspond to the same halo-to-total mass ratio.

the above analysis is valid only for the merging of two galaxies in a cluster consisting of a large number of galaxies. Nevertheless, the above theoretical analysis, albeit very simplified, gives some insight to our result and argues that our result is not surprising and that the lifetime should depend only weakly on the size of the galaxies.

5.2 Common halos

Figures 4 and 5 compare merging rates for groups with common halos and different percentages of halo masses. We note that the higher the halo mass, the slower the merging

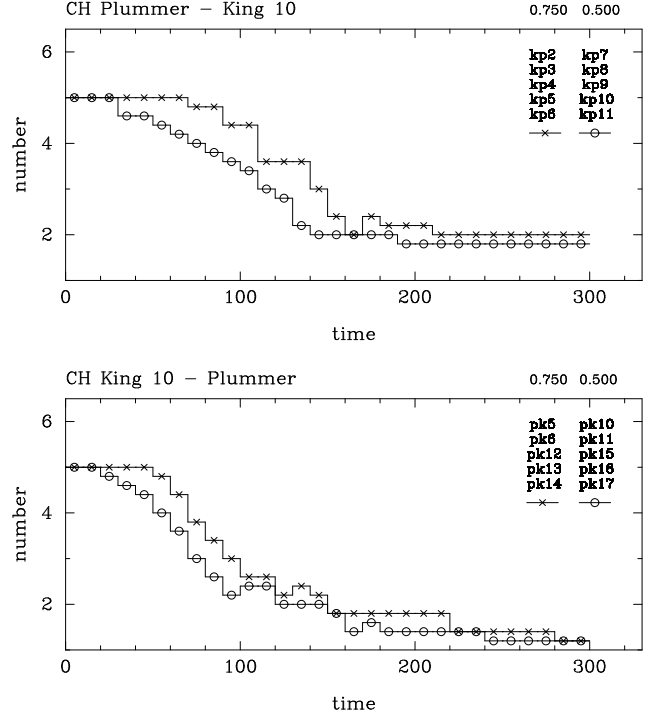


Figure 5. As for the previous figure, but for King $\Psi = 10$ groups in Plummer common halos (upper panel) and for Plummer groups in King $\Psi = 10$ common halos (lower panel). The different symbols correspond to the same halo-to-total mass ratio (circles for 0.5 and crosses for 0.75). It is clear from this and the previous figure that groups with relatively more massive common halos merge slower than groups with less massive common halos, and that independent of the model of the group or halo (King or Plummer).

will occur and this independent of whether the distribution of the galaxies and the halo are Plummer, King $\Psi = 10$, or King $\Psi = 1$. It is also true for mixed distributions, i.e. King $\Psi = 10$ groups in Plummer halos, or Plummer groups in King $\Psi = 10$ halos. This result can be best understood if we think of the galaxies as a perturbation on the global halo potential. If the halo-to-luminous mass ratio is small, the perturbations will be larger, the galaxies will be strongly attracted by each other and will merge faster. The opposite will be true for the case of large halo-to-luminous mass ratios. In the limiting case where the galaxies are test particles in the common halo they will merge only if their mutual trajectories intersect accidentally.

We can reach the same conclusion using arguments similar to those of the previous section. Let us again consider two groups consisting of galaxies with the same size and with different masses m_1 and $m_2 = km_1$ respectively. We then have

$$\sigma(v, m_2) = \sigma(vk^{-1/2}, m_1), \quad (12)$$

instead of (7). In this case, following a derivation similar to that in the previous section, we have

$$P_2 \sim \begin{cases} P_1 k^2, & (\sigma_{group} \gg \sigma_{gal}) \\ P_1 k^{4/3}, & (\sigma_{group} \ll \sigma_{gal}) \end{cases} \quad (13)$$

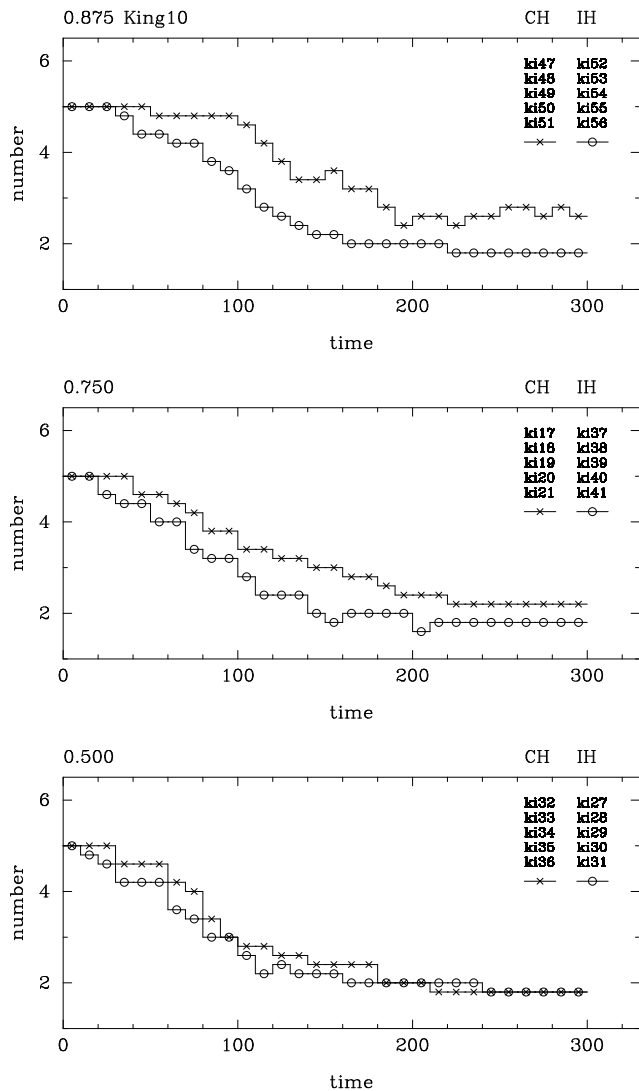


Figure 6. Number of galaxies as a function of time for King $\Psi = 10$ groups. The upper panel corresponds to a halo-to-total mass ratio of 0.875, either in a common halo (crosses), or in individual halos (squares). The middle panel corresponds to a halo-to-total mass ratio of 0.75 and the lower one is for a halo-to-total mass ratio of 0.5, while the symbols are the same as for the upper panel. We note that the merging rate for models with individual halos is always higher than that for models with common halos, the difference being larger with increasing halo-to-total mass ratio.

Thus, in both limits, the lifetime should depend relatively strongly on the mass of the galaxies and in the same sense as found by the numerical simulations.

5.3 Individual versus common halos

Fig. 6 shows the behaviour of models with King distributions of index $\Psi = 10$. The merging rate for models with individual halos is higher than that for models with common halos and this for all halo-to-total mass ratios and independent of the number of the remaining galaxies in the group. This is in good agreement with the results of Barnes

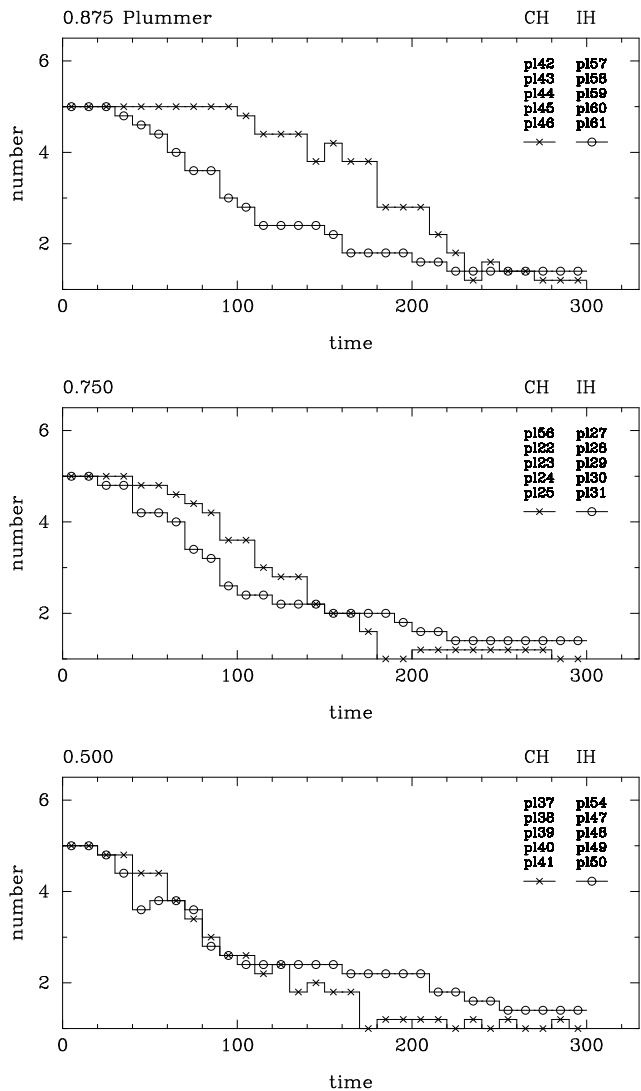


Figure 7. As for figure 6, but now for Plummer groups. We note that the evolution is faster initially for individual halo cases, then there is a cross-over and it is the common halo cases that merge faster. Where the cross-over occurs depends on the halo-to-total mass ratio.

(1985) and Bode, Cohn & Lugger (1992), who also use King distributions for the group and halo, albeit for $\Psi = 7$, and different model galaxies.

Figure 7 compares again merging rates of groups with common halos to groups with individual halos, but now for Plummer groups and, whenever relevant, Plummer common halos. In the upper panel, corresponding to a halo-to-total mass ratio of 0.875, we see that the merging goes considerably faster for groups with individual halos. The behaviour is more complicated for halo-to total mass ratio of 0.75 or 0.5. Initially the number of mergers in the simulations with individual halos is larger than that in the simulations with common halos. The trend, however, is reversed after some time and configurations with common halo show much larger merger rates than those with individual ones, due to the fact that the configurations with common halos develop some

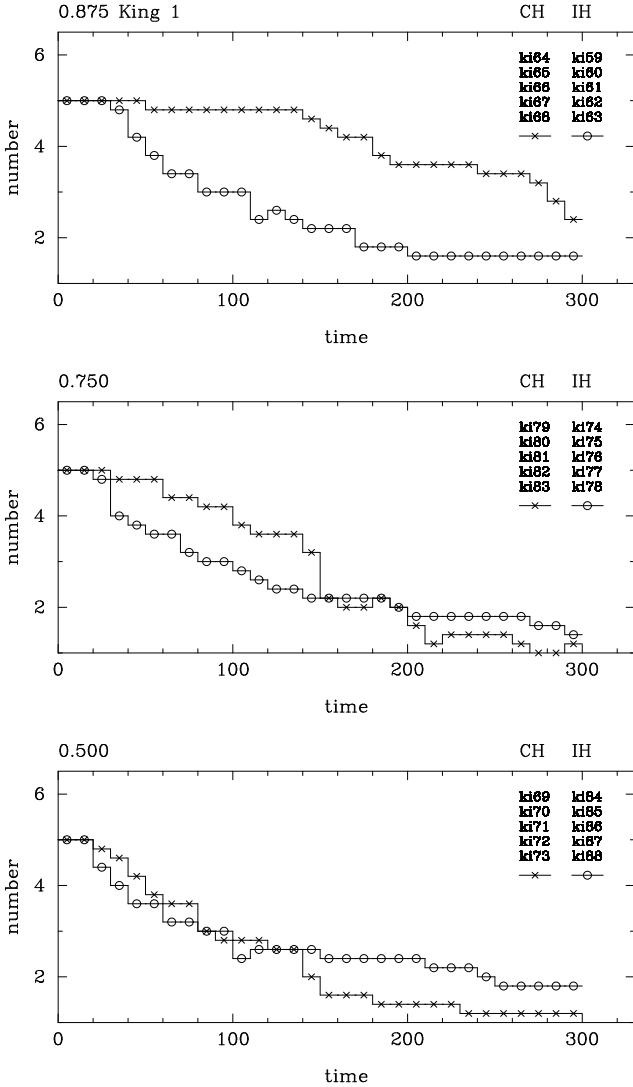


Figure 8. As for Figure 7, but now for King $\Psi = 1$ groups.

longer lived binary or triplet configurations than the common halo cases. This cross-over occurs roughly when 2 galaxies are left in the group for a halo-to-total mass ratio of 0.75 and at 3 galaxies for a 0.5 mass ratio. Since Athanassoula & Makino (1995) were only discussing the time of final total merge, these two panels show a behaviour in good agreement with their results, which is not surprising since they also used Plummer distributions.

Figure 8 shows similar plots, but now for King $\Psi = 1$ profiles. The results are very similar to those found for Plummer distributions, in the sense that for halo-to-total mass ratios of 0.75 and 0.5 the curves cross over, so that initially the merging rate is higher in the case of individual halos, the opposite being true for later times. Furthermore the cross-over positions, in terms of galaxies left in the group, are roughly the same for Plummer and King $\Psi = 1$ profiles.

There are two effects influencing the merging rate in an opposite sense. On the one hand in the case of individual halos the mutual attraction between galaxies is highest and that should favour faster merging. On the other hand a dense

common halo entails an important dynamical friction and a corresponding slow-down of the galaxies, thus also favouring fast merging. It seems that the first effect dominates in the case of King $\Psi = 10$ groups and in the initial stages of the evolution of Plummer and King $\Psi = 1$ groups, and the second one in the remaining cases. This can be understood as follows: In the initial stages of the simulations the galaxies are relatively far apart, therefore mutual attractions are important to help them come near each other and merge. Later in the evolution the half-mass radius of the luminous material has shrunk considerably and galaxies are very near each other. Thus mutual attractions are not that important anymore, while dynamical friction slows the galaxies down and speeds up the merging process. This, however, is not true for King $\Psi = 10$ models, since, as was discussed in section 4, the distribution of the merging positions reflects the initial distribution of the galaxies. Therefore for King $\Psi = 10$ models several mergings occur relatively far from the center and the mutual attractions are still important to stimulate encounters.

5.4 Effect of different distributions

Let us now discuss the effect of central concentration on the merging rate. In the case of individual halos, comparing simulations with different distribution of the galaxies in the group, we see that there is a tendency for groups distributed in a more homogeneous way to merge faster during the last parts of the simulation. The effect, however, is very small. The comparison for cases with common halos can be seen in fig. 9. For low and intermediate halo-to-total mass ratios (upper and middle panels) the comparison goes as for simulations with individual halos, although the effect of central concentration is somewhat stronger. The first few mergings happen quite early on and that independent of the central concentration. The last mergings occur much later in the case of King 10 distributions than in the others.

The effect of central concentration is most clearly seen for the higher halo-to-total mass ratio (lower panel). It is the least centrally concentrated configuration, namely the King $\Psi = 1$ one, that merges the slowest. Since central concentration does not affect much the merging rates in simulations with individual halos, we infer that it is the central concentration of the common halo that makes the difference in this case. Then the observed behaviour can be explained as follows: For the case of not centrally concentrated halos one can see that the galaxies oscillate in the common halo potential, influenced little by their mutual attractions, and slowed down by dynamical friction. One can consider such motions as damped oscillations, but with a relatively small damping factor, since the mass in the halo is distributed over a large volume so that the density, even for large halo-to-total mass ratios, is not very high. This is not the case for centrally concentrated halos. Now the dynamical friction is small when the galaxy is in the outer parts of the halo, and much bigger in the inner parts, particularly so when the galaxy has the high concentration parts behind it. In other words the galaxy is very heavily decelerated after it just crossed the center and, because of the energy it loses, it settles in the central parts of the potential well, so that mergings occur easier. Thus galaxies merge faster in more centrally concentrated common halos.

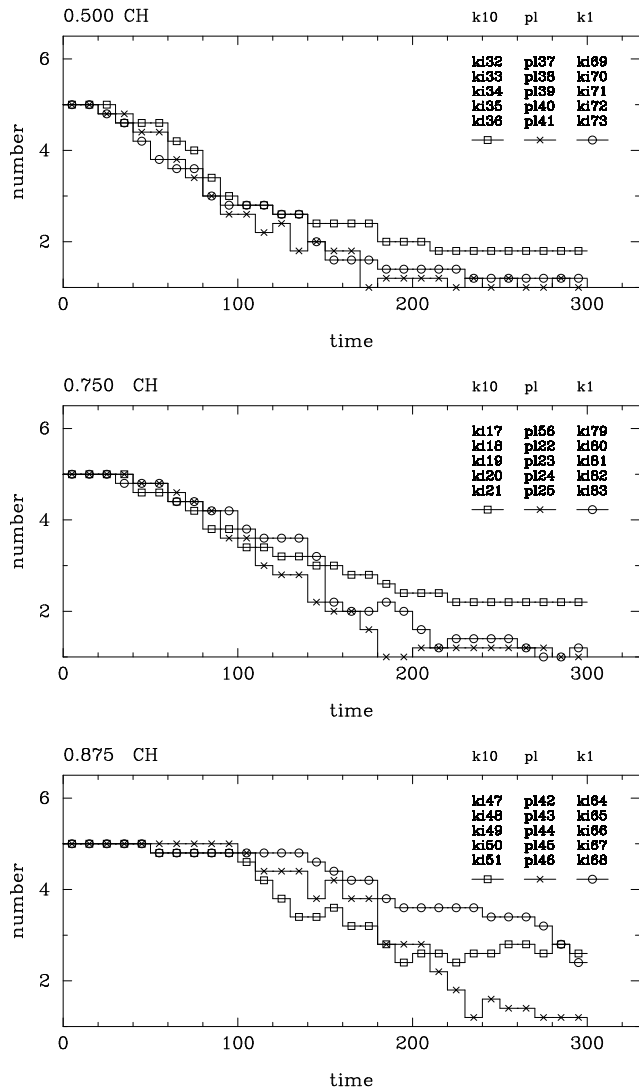


Figure 9. Number of galaxies as a function of time for simulations with common halos and a halo-to-total mass ratio of 0.5 (upper panel), 0.75 (middle panel) and 0.875 (lower panel). The most centrally concentrated configuration (King $\Psi = 10$, squares), is compared to an intermediate one (Plummer, crosses) and to the least centrally concentrated (King $\Psi = 1$, circles).

To illustrate this we follow the motion of a galaxy in a common halo, which is either King $\Psi = 1$ or King $\Psi = 10$. In both examples the galaxy starts off at $t = 0$ from $x = 50$ and has no initial velocity. The ratio of the galaxy-to-total mass is 0.025. In figure 10 we plot the distance of the galaxy from the center of the common halo as a function of time. The center of the galaxy can be either defined from its densest part (solid line), or its center of mass (dashed line). In the case of the King $\Psi = 1$ common halo the galaxy does not suffer a serious deformation, nor does it lose much of its mass. Thus the maximum density point does not differ significantly from the center-of-mass. The galaxy oscillates around the center of the halo, while being slowly decelerated by dynamical friction. It takes longer than $t = 550$, or equivalently more than 3.5 oscillations, before it is im-

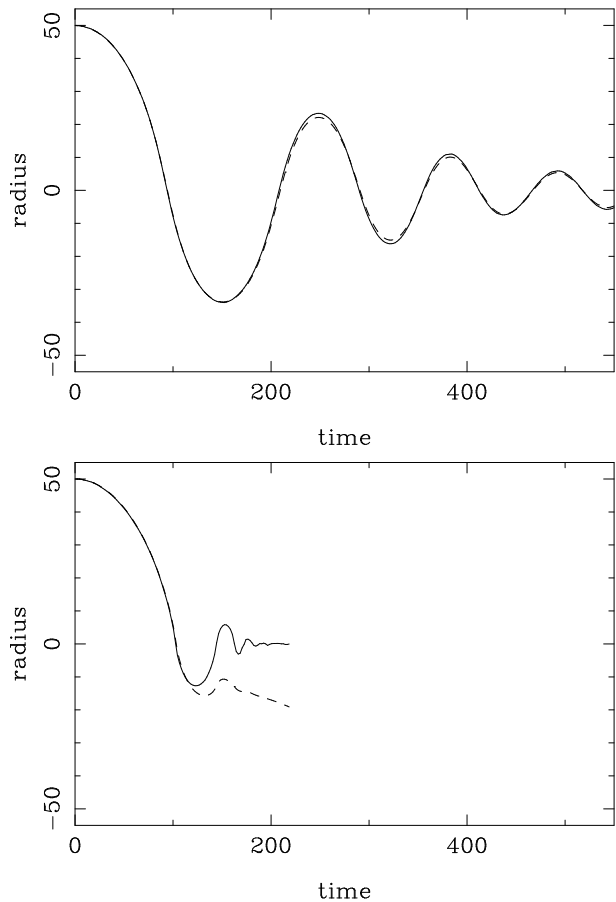


Figure 10. Distance of the center of a galaxy from the center of the common halo - which is either a King $\Psi = 1$ (upper panel), or a King $\Psi = 10$ (lower panel). The center of the galaxy is obtained either from its center of mass (dashed line) or from its highest density point (solid line). The simulation is described in the text.

bilised in the central part of the halo. The situation is very different in the case of a King $\Psi = 10$ common halo. Now the galaxy suffers severe distortions when it goes through the halo center and loses a considerable fraction of its mass, starting from its first passage through the halo center. Thus the center of mass of the galaxy does not coincide with the point of maximum density. Following the latter, which is a more reasonable definition of the galaxy center, we see that the galaxy is decelerated in the central regions of the halo, loses an important fraction of its kinetic energy and can not reach the outer parts of the halo any more. This happens at relatively early times, before $t = 200$. Staying in the inner parts it would, had other galaxies been presented in the simulation, be an easy prey to merging. Thus merging should proceed faster in centrally concentrated common halos.

5.5 Different initial kinematics

5.5.1 Cylindrically rotating groups

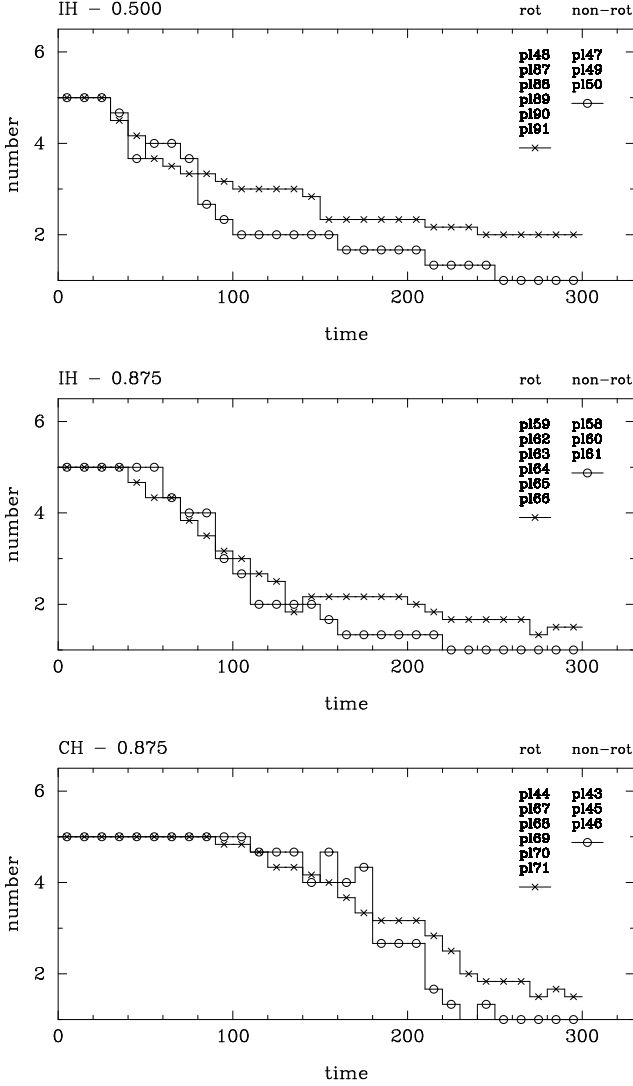


Figure 11. The effect of cylindrical rotation on the merging rate. The average of cylindrically rotating groups is given by crosses and of non-rotating ones by circles. The comparison is done for individual halo cases (upper two panels) and common halo ones (lower panel). The halo-to-total mass ratios considered are 0.5 (upper panel) and 0.875 (middle and lower panels).

Our runs allow us to make three different comparisons between cylindrically rotating and non-rotating groups, for different halo mass distributions and ratios, and we show them in Figure 11. The initial conditions for the cylindrically rotating groups were generated as described in section 2, namely by orienting the velocity vector of the mean velocity of each galaxy in the (x, y) plane so that it is perpendicular to the cylindrical radius of the galaxy. These will be compared with initial conditions where this velocity vector is randomly oriented. It happened, however, that, out of the initial conditions generated with random orientation of the velocities, one had a substantial amount of cylindrical rotation around the z -axis, so should be included in the group of the fast z -rotators, while another one was an intermediate z -rotator, and thus was left out of the comparisons. We

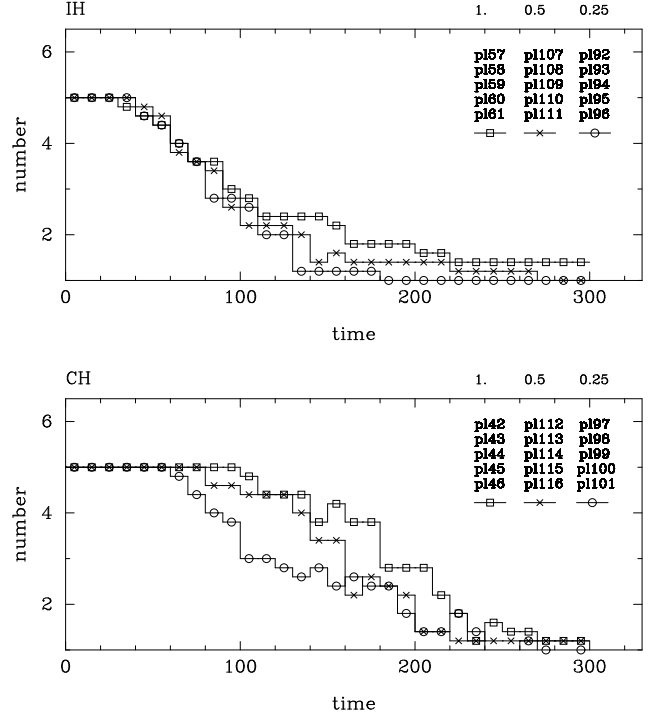


Figure 12. Number of galaxies as a function of time for simulations starting with $2T/|W| = 0.25$ (circles), with $2T/|W| = 0.5$ (crosses) and with $2T/|W| = 1$ (squares). The upper panel corresponds to simulations with individual halos and the lower one to simulations with common halos. The halo-to-total mass ratio is 0.875 in all cases.

will thus be comparing in all cases 6 groups of galaxies with fast cylindrical rotation around the z -axis with 3 groups of galaxies with slow rotation. As shown in Figure 11 there is a clear indication that faster cylindrically rotating groups take longer to merge than slower ones, as expected. The effect, however, is not very large.

5.5.2 Cold groups

Cold groups are more extended and have a smaller velocity dispersion. They start out of equilibrium, so they initially undergo a rapid collapse and a heating. Eventually, after some oscillations, their virial ratio reaches values around unity. At that time, provided merging does not hinder comparisons, the bulk velocities of the individual galaxies seem to be somewhat smaller than for the galaxies initially in virialised groups.

Figure 12 compares the number of galaxies left at a given time in groups in virial equilibrium ($2T/|W| = 1$) with that of cold groups ($2T/|W| = 0.25$ and 0.5). The upper panel corresponds to groups with individual halos and the lower one to groups with common halos; in all cases the halo-to-total mass ratio is 0.875. We see that cold groups merge faster than the ones in virial equilibrium, as could be expected since encounters happen at smaller relative velocities and the angular momentum of the galaxies is in general smaller (cf. preceding section). Comparing the two panels

we also note that the difference between virial and collapsing groups is more important in the case of common halos than in the case of individual ones.

In Fig. 12 we plot the number of galaxies as a function of times, as we did in all other cases. If, however, we measured time not in computer units but in multiples of some suitably defined initial crossing time, the difference between cold and virialised groups would be more important. This comes from the fact that cold groups are more extended and have lower bulk galaxy velocities, i.e. have larger crossing times.

5.5.3 Expanding groups

There is not much difference in the merging rates of expanding groups with individual halos from those of the corresponding non-expanding ones, except for the last stages of the evolution. In the last stages the final pair survives longer and can often be unbound. This is due to the fact that, due to the Hubble flow initial conditions, the galaxy that is furthest from the center has a substantial outwards velocity and takes some time before turning around, if it ever does. On the other hand the galaxies that are in the central areas have similar merging histories as in the non-expanding cases. The effect of a Hubble expansion would presumably have been more important if the galaxies were initially less concentrated and located more in the outer parts, but we have not run such cases.

Expanding groups with common halos merge faster than virialised groups with common halos. This effect is probably due to our initial conditions. Indeed the initial configuration is not in equilibrium, and the common halo evolves very fast towards a more concentrated triaxial configuration. The galaxies respond to this - as well as to the instability of their own configuration - and find themselves focused towards the inner parts, particularly in the direction of the minor and median axes of the halo. Thus encounters and subsequent mergers are favoured and the merging rates are higher than in simulations starting off near equilibrium. Obtaining initial configurations which have a Hubble expansion and start near a stable equilibrium is beyond the scope of this paper.

6 PAIRS AND TRIPLETS

All the 35 simulations with galaxies distributed according to Plummer models listed in Table 3 have merged before $t = 500$. On the other hand out of 45 King $\Psi = 10$ configurations 8 become unbound triplets, while another 8 pairs and 1 quartet have not merged although we have continued the simulations for very long times, roughly up to $t = 1000$. In all cases they come from two starting conditions, the second, which we will hereafter call condition B, and the third which we will call condition C. The reason is that, as we saw in section 2.1, the King $\Psi = 10$ model has a rather extended outer halo, so that occasionally points will be drawn relatively far from the others. This is the case for configuration C, where the fifth galaxy is initially far from the other four. For the four cases with individual halos this configuration ends up as an unbound triplet, two of its members having roughly twice the mass of the third one. The simulations starting with configuration C and having common halos neither merge by the

end of the simulations, nor do they become unbound, but end up as bound pairs, presumably to merge at times much larger than 1000.

Configuration B is a similar case, where all five galaxies are initially relatively far apart. For the four cases with individual halos the configuration ends up as an unbound triplet. Four of the simulations with common halos neither merge by the end of the simulations, nor do they become unbound, but three end up as bound pairs and one as a bound quartet. Two of the pairs have a mass ratio of 3:2 and one of 4:1. The fifth case with common halo merged fully at $t = 1030$.

Groups with King $\Psi = 1$ or 5 distributions give no unbound final cases, although 1 of the 15 King $\Psi = 5$ cases and 3 of the 30 King $\Psi = 1$ did not merge fully by $t = 1000$.

7 HOW TO GET COMPACT GROUPS WHICH MERGE SLOWLY

The aim of our simulations was, given a system of five galaxies with a given total mass and energy, to find which configurations have the lowest merging rates. We consider both cases with individual halos and cases where the halo is common, enveloping the whole group. In the latter cases the merging rate is slower for cases where the halo is more massive. On the other hand the mass of individual halos does not influence much the merging rates, due to the fact that all galaxies have the same mass, and so more extended ones have a smaller velocity dispersion. Groups with individual halos merge faster than groups with common halos if the configuration is centrally concentrated, like a King distribution of index $\Psi = 10$. On the other hand for less concentrated configurations the merging is initially faster for individual halo cases, the reverse being true after part of the group has merged. In cases with common halo centrally concentrated configurations merge slower for low halo-to-total mass ratios and faster for high mass ratios. Groups which have initially a virial ratio which is less than one merge faster, and groups that have initially cylindrical rotation merge slower than groups starting in virial equilibrium.

Led by the above, we have tried to find one simulation which would have very slow merging rates. For simplicity we have restricted ourselves to cases initially in virial equilibrium, though if we waive this restriction we can get even longer lived configurations. Our simulations led us to try a case with a high halo-to-total mass ratio, distributed in a common halo which is as homogeneous as possible. In order to build such a halo we followed the evolution of a truncated homogeneous sphere composed of 155325 particles for 30 time units, a time sufficient for quasi equilibrium to be reached. We added 5 galaxies - composed of 1635 particles each - with initial mean positions and velocities drawn at random from the particles constituting the common halo, rescaled appropriately so that the simulation would start in equilibrium and represent a compact group in virial equilibrium and with a ratio of common halo mass to total mass of 0.95. We evolved this in the same way as all the other simulations. The striking result is that the first merging occurred only at $t = 990$, followed closely by the subsequent mergings at $t = 1010, 1060$ and 1110 respectively. This is considerably longer than corresponding times for other simulations. (This

simulation took 32 days on the Marseille GRAPE-3AF system). For comparison let us note that for simulations with individual halos starting off in virial equilibrium the mean times for the four mergings are roughly 60, 85, 145 and 243 respectively. If we use as length the radius containing 80% of the halo mass at $t = 0$ and as velocity the value $1/\sqrt{2}$, then we get a measure of the crossing time roughly equal to 34. This means that the four mergings in this simulation occurred after roughly 29, 30, 31 and 33 crossing times.

Converting times to astronomical units is neither straightforward nor unique. On the one hand observations give us estimates of the velocity dispersion in the group now, and not at the beginning of the evolution. Also, for a fairer comparison, the mass of the group should include the halo mass within the volume occupied by the galaxies at the beginning of the evolution and not now. Nevertheless we can try a rough estimate. Thus using for a group mass $10^{13} M_{\odot}$ and for the velocity dispersion 300 km/sec we get that a 1000 computer units for time correspond roughly to 28 Gyrs. Considering a smaller mass for the group or a larger velocity dispersion would of course reduce this value.

This value is sufficiently large to allow us to conclude that a compact group such as described in this section can survive for a time comparable or larger to the age of the universe. It should also be noted that the value of common-halo-to-total mass ratio used in this example is not excessive. Pildis, Bregman & Evrard (1995) have analysed a sample of 12 HCGs plus the NGC 2300 group. For those groups that have extended X-ray emission, i.e. approximately two-thirds of the sample, they find a baryon fraction between 5% and 19%. If we take into account that the hot gas component contributes part of the baryons, while in our analysis it would contribute to the common halo mass, we see that the mass fraction we adopted is not unreasonable. Furthermore, as we already mentioned, some more longevity could be obtained if we also use the most favourable kinematical initial conditions, rather than limiting ourselves to virial equilibrium by default.

Thus our simulations point to a third solution to the compact group problem, providing an alternative explanation for why we observe so many compact groups despite the fact that their lifetimes are believed to be so short. Namely it could be that the groups we observe have survived because they have a common halo, of considerable mass, distributed in an appropriate way, and/or have appropriate kinematical initial conditions. The other solutions proposed so far are that the compact groups are not real entities, but chance projections of at least some members of the group (e.g. Rose 1979; Mamon 1986, 1987, 1995; Hernquist, Katz & Weinberg 1994); and that they continuously form as subunits of rich groups (e.g. Diaferio, Geller & Ramella 1994). In order to discuss seriously these three alternatives and their implications we first have to make a thorough analysis of the structure and kinematics of the merger remnants, which we will do in a future paper.

Finally let us note that our simulations have not been done within a cosmological context and that, despite the large number of simulations tried (over 250) many effects have not been addressed. Thus all our initial conditions have been drawn from distributions which are spherically symmetric, isotropic, isolated and devoid of gas, and all galaxies are equal mass spherical ellipticals. Some of these assump-

tions will certainly influence the merging rates and it could be that their effect could further prolong the lifetime of a group. Such a study, however, is beyond the scope of this paper.

ACKNOWLEDGEMENTS

We would like to thank Jean-Charles Lambert for his help with the administration of the simulations. E. A. and A. B. gratefully acknowledge the hospitality of the College of Arts and Sciences of the University of Tokyo and CNRS-JSPS exchange grants which made their trips possible. They would also like to thank the INSU/CNRS and the University of Aix-Marseille I for funds to develop the computing facilities used for the calculations in this paper. J. M. gratefully acknowledges the hospitality of the Observatoire de Marseille and CNRS-JSPS exchange grants which made his trips possible. The NEMO package was often used both in the generation of the initial conditions and the analysis of the simulations and we are indebted to Peter Teuben for his efforts to maintain it.

REFERENCES

- Athanassoula E., Makino J., 1995, in *Groups of Galaxies*, eds. O. Richter, K. Borne, A.S.P. conf series No. 70, p. 143
 Barnes J. E., 1985, *MNRAS*, 215, 517
 Barnes J. E., 1992, *ApJ*, 393, 484
 Bode P. W., Cohn H. N., Lugger P. M., 1992, *ApJ*, 416, 17
 Casertano S., Hut P., 1985, *ApJ*, 298, 80
 Cavaliere A., Santangelo P., Tarquini G., Vittorio N., 1982, in *Clustering in the Universe*, eds. D. Gerbal, A. Mazure, p. 25, Editions Frontieres, Gif sur Yvette
 Ciotti L., 1996, Preprint (astro-ph 9605084)
 Diaferio A., Geller M. J., Ramella M., 1994, *AJ*, 107, 868
 Governato F., Bhatia R., Chincarini G., 1991, *ApJL*, 371, L18
 Ebisuzaki T., Makino J., Fukushige T., Taiji M., Sugimoto D., Ito T., Okumura S. K., 1993, *PASJ*, 45, 269
 Hernquist L., Katz N., Weinberg D., 1995, *ApJ*, 442, 57
 Hickson P., 1982, *ApJ*, 255, 382
 Hickson P., Mendes de Oliveira C., Huchra J. P., Palumbo G. G. C., 1992, *ApJ*, 399, 353
 von Hoerner S., 1963, *Z. Ap*, 57, 47
 Makino J., Hut, P., 1996, preprint
 Mamon G. A., 1986, *ApJ*, 307, 426
 Mamon G. A., 1987, *ApJ*, 321, 622
 Mamon G. A., 1995, in *Groups of Galaxies*, eds. O. Richter, K. Borne, A.S.P. conf. series No. 70, p 83
 Navarro J., Mosconi M. B., Garcia Lambas D., 1987, *MNRAS*, 228, 501
 Okumura S. K., Makino J., Ebisuzaki T., Ito T., Fukushige T., Sugimoto D., Hashimoto E., Tomida K., Miyakawa N., 1992, in *Proceedings of the twenty-fifth Hawaii International Conference on System Sciences*, I, 151
 Okumura S. K., Makino J., Ebisuzaki T., Fukushige T., Ito T., Sugimoto D., Hashimoto E., Tomida K., Miyakawa N., 1993, *PASJ*, 45, 329
 Pildis R. A., Bregman J. N., Evrard A. E., 1995, *ApJ*, 443, 514
 Rose J. A., 1979, *ApJ*, 231, 10
 Weil M. L., Hernquist L., 1994, *ApJ*, 431, L79
 Weil M. L., Hernquist L., 1996, *ApJL*, 460, 101
 White S., 1979, *MNRAS*, 189, 831

This paper has been produced using the Royal Astronomical Society/Blackwell Science L^AT_EX style file.